Published in final edited form as:
Brain Behav Immun. 2014 February ; 36: 61–70. doi:10.1016/j.bbi.2013.10.008.

Cell-autonomous iodothyronine deiodinase expression mediates seasonal plasticity in immune function

Tyler J Stevenson[†,*], **Kenneth G Onishi**[†], **Sean P Bradley**[†,‡], and **Brian J Prendergast**[†,‡]
[†]Institute for Mind and Biology, University of Chicago, Chicago IL, USA, 60637
[‡]Department of Psychology, University of Chicago, Chicago IL, USA, 60637

Abstract

Annual rhythms in morbidity and mortality are well-documented, and host defense mechanisms undergo marked seasonal phenotypic change. Siberian hamsters (*Phodopus sungorus*) exhibit striking immunological plasticity following adaptation to short winter day lengths (SD), including increases in blood leukocytes and in the magnitude of T cell-mediated immune responses. Thyroid hormone (TH) signaling is rate-limited by tissue-level expression of iodothyronine deiodinase types II and III (*dio2*, *dio3*), and *dio2*/*dio3* expression in the central nervous system gate TH-dependent transduction of photoperiod information into the neuroendocrine system. THs are also potent immunomodulators, but their role in seasonal immunobiology remains unexamined. Here we report that photoperiod-driven changes in triiodothyronine (T_3) signaling mediate seasonal changes in multiple aspects of immune function. Transfer from long days (LD) to SD inhibited leukocyte *dio3* expression, which increased cellular $T_4 \rightarrow T_3$ catabolism. T_3 was preferentially localized in the lymphocyte cytoplasm, consistent with a non-nuclear role of T_3 in lymphoid cell differentiation and maturation. Exposure to SD upregulated leukocyte DNA methyltransferase expression and markedly increased DNA methylation in the *dio3* proximal promoter region. Lastly, to bypass low endogenous T_3 biosynthesis in LD lymphocytes, LD hamsters were treated with T_3, which enhanced T cell-dependent delayed-type hypersensitivity inflammatory responses and blood leukocyte concentrations in a dose-dependent manner, mimicking effects of SD on these immunophenotypes. T_3 signaling represents a novel mechanism by which environmental day length cues impact the immune system: changes in day length alter lymphoid cell T_3-signaling via epigenetic transcriptional control of *dio3* expression.

Keywords

thyroid; photoperiod; hamster; cytometry; rhythm; adaptive immunity; imaging flow cytometry

[*]Corresponding Author: Tyler J. Stevenson, Ph.D., Institute of Biological and Environmental Sciences, University of Aberdeen, Aberdeen, UK AB24 3FX, tyler.stevenson@abdn.ac.uk, telephone: 01224 274145.

This report identifies cell-autonomous (lymphocyte) thyroid hormone catabolism as the mechanism by which seasonal changes in day length regulate immune function.

INTRODUCTION

In human and non-human populations, immune function changes markedly over daily and seasonal timescales (Nelson, 2004; Bilbo et al., 2002). Whereas central and peripheral circadian clocks have been identified as key physiological mechanisms responsible for generating diurnal rhythms in immune function (Prendergast et al., 2013a; Logan and Sarkar, 2012; Bechtold et al., 2010), the proximate causes of seasonal cycles in immunity have yet to be identified. Siberian hamsters (*Phodopus sungorus*) are a canonical model for the investigation of seasonal physiological rhythms (Prendergast et al., 2009). Changes in day length (photoperiod) are sufficient to induce widespread alterations in innate and adaptive immunity. Following exposure to short, winter-like photoperiods (SD), hamsters exhibit complete regression of the reproductive system; in parallel, multiple aspects of immune function adopt a winter phenotype: blood leukocyte subpopulations and delayed-type hypersensitivity (DTH) inflammatory responses are enhanced, whereas infection-induced proinflammatory cytokine production, fever, and sickness behaviors are markedly inhibited (Nelson, 2004). Enhancements in blood lymphocyte function and in T cell mediated responses are critical for long-term adaptive immune function during the winter (Nelson, 2004; Walton et al., 2011). Photoperiod-driven changes in nocturnal melatonin secretion are necessary and sufficient for generating seasonal changes in nearly all aspects of immunity studied to date (Yellow et al., 1999; Wen et al., 2007; Freeman et al., 2007); but seasonal changes in gonadal hormone secretion do not fully account for annual cycles in immunity (Prendergast et al., 2008; Prendergast et al., 2005). The amplitude of seasonal changes in numerous measures of immunity in hamsters encompasses a range that would be clinically diagnostic of an immunocompromised state in humans (Nelson 2004, Bechtold et al., 2010; Walton et al., 2011), yet hamsters exhibit this reversible seasonal plasticity in the immune system in the absence of comorbid illness.

Thyroid hormone signaling plays a central role in photoperiod-driven regulation of reproductive physiology (Yasuo and Yoshimura, 2009). Triiodothyronine (T_3) enhances GnRH signaling to the pituitary via morphological changes in neuro-glial interactions in the median eminence (Yamamura et al., 2004). Systemic levels of the prohormone thyroxine (T_4) do not vary seasonally (O'Jile and Bartness, 1992), but changes in day length markedly alter the expression of iodothyronine deiodinases (DIOs) in the hypothalamus (Yoshimura et al., 2003; Nakao et al., 2008; Barrett et al., 2007; Ono et al., 2008; Prendergast et al., 2013b). Long, summer-like photoperiods (LDs) increase hypothalamic DIO2 expression, which converts T_4 into the receptor-active T_3 and enhances T_3 signaling, whereas SDs increase DIO3 expression, which converts T_4 into the biologically-inactive enantiomer, rT_3, and thereby quenches T_3 signaling (Yoshimura et al., 2003; St Germain et al., 2009; Bianco et al., 2002). In sum, photoperiod information is transduced into the reproductive system via DIO-mediated catabolism of T_4, and changes in day length create local thyroid hormone microenvironments in the hypothalamus that effectively gate gonadotropin secretion (Yoshimura et al., 2003).

Thyroid hormones are also potent immunomodulators (Dorshkind and Horseman, 2000), yet a role for T_3 signaling in the genesis of seasonal changes in immunity has not been examined. Thyroid hormone receptors (TRs) are expressed in most lymphoid tissues (Sengal and Ingbar, 1982; Foster et al., 1999), and T_3 modulates of lymphoid cell development and immune function (Mascanfroni et al., 2008; 2010). Thymopoesis is markedly reduced in hypothyroid mice (Alpin et al., 2000), as is maturation of B cells (Murphy et al., 1992), both of which are restored by T_4 therapy (Montecino-Rodriguez et al., 1996). Innate immune responses to *Listeria* are suppressed in hypothyroid mice (Foster et al., 2000). In euthyroid mouse and rat models, maturation and activation of antigen-presenting dendritic cells are dependent on non-nuclear (cytosolic) T_3 signaling (Mascanfroni et al., 2008; 2010), and

supplemental T_4/T_3 treatments enhance T cell-dependent skin immune responses (Chandel and Chatterjee, 1989) and alter mitogen-induced proliferation of blood-, thymus-and spleen-derived leukocytes (Chatterjee and Chandel, 1983).

These experiments examined whether photoperiod-driven changes in thyroid hormone signaling impart seasonal time information into the immune system. Experiments quantified effects of photoperiod on *dio2* and *dio3* mRNA expression in blood leukocytes, and specified a role for epigenetic mechanisms in the regulation of lymphoid cell *dio2/dio3* expression by photoperiod. Photoperiod effects on $T_4 \rightarrow T_3$ catabolism and on cellular compartmentalization T_3 were also examined, and *in vivo* experiments tested the hypothesis that T_3 treatment could mimic effects of photoperiod on constitutive and adaptive immunity.

MATERIALS and METHODS

Subjects

Male and female Siberian hamsters (*Phodopus sungorus*) were selected from a colony maintained at the University of Chicago. Hamsters were housed in polypropylene cages illuminated for 15 h per day (15L:9D). All procedures were approved by the Animal Care and Use Committee at the University of Chicago.

Experiments

Study 1: SD induced changes in leukocyte concentrations and mRNA expression—To examine the effects of acute exposure to inhibitory short day lengths (SD; 9h light/day; lights off at 1700h CST) male and female hamsters were either housed in the colony LD photoperiod (15L:9D ; n=13 M; 11 F) or in SD (9L:15D ; n=10 M; 10 F) for 10 weeks. Hamsters were anesthetized with isoflurane gas (4%) and 500μl whole blood was obtained via the right retroorbital sinus using sterilized Pasteur pipettes coated with sodium heparin. A 25 μl aliquot was mixed with 3% acetic acid at a 1:20 dilution (Unopette, Beckton-Dickinson). Total leukocyte numbers were counted according to methods previously reported (Prendergast et al., 2003). Leukocytes were then isolated from the blood via osmotic lysis followed by DNA/RNA extraction (see below). Gonadal state was assessed as previously described (Prendergast et al., 2013b).

DNA/RNA isolation: Leukocyte DNA/RNA were extracted using QIAGEN AllPrep DNA/RNA mini kit following the manufacturer's instructions. DNA and RNA concentration and quality were determined by spectrophotometer (Nanodrop, Thermo Scientific Wilmington, DE). cDNA was synthesized using Superscript III (Invitrogen, Carlsbad, USA) and genomic DNA and cDNA were stored at −20°C.

Quantitative PCR (qPCR) for gapdh, dio2, dio3, and dnmts: qPCRs were performed using a BIORAD CFX384 system using the following steps i) an initial denature at 95°C for 30 secs, then 39 cycles of ii) 95°C for 10 sec, iii) annealing dependent on target mRNA (See Table S1) for 30 secs and then iv) an extension at 72°C for 30 sec. The specificity of select samples was established by resolving PCR products in 2.5% agarose gel. A melting curve analysis was added to determine the quality and specificity of each reaction. Quantification of mRNA expression levels was accomplished with iQ Sybr Green Supermix (BIORAD, Hercules, USA). We used PCR Miner (Zhao and Fernald, 2005) to calculate reaction efficiencies (E) and cycle thresholds (CTs). The average E for all reaction was close to 1.0 and samples that were below 0.8 or above 1.2 were excluded from analyses. The expression of each target gene of interest relative to *gapdh* was determined using $2^{-(\text{delta-deltaCt})}$.

Methylation-sensitive restriction enzyme assay (MSRE): Leukocyte DNA from all hamsters was subjected to MSRE analyses. The restriction enzymes, *Hpall* and *BstUl* were selected to cleave the *dio3* promoter region at 4 distinct regions within the region amplified during PCR. These enzymes can only cut DNA sequences (CCGG and CGCG, respectively) that are not methylated, and leave methylated DNA intact. Therefore, DNA that is unmethylated will be cut and therefore, resulted in lower levels of PCR amplification. 250ng of genomic DNA was placed into two tubes: an enzyme treated + buffer and a no-enzyme + buffer control. The tubes were then processed using the primers (Table S1) surrounding the targeted CpG sites with the no-enzyme control serving as a reference. 1μl of each enzyme and 1μl NEB buffer 1 (New England Biolabs, Ipswich, MA) was added to the tubes, water was added to obtain a final volume of 25μl. Samples were then incubated at 37°C for three hours. Control samples included: no-DNA with enzyme and no-DNA and no-enzyme. *Hpall* and *BstUl* were inactivated by incubation at 65°C for 20 minutes. qPCRs were performed using a BIORAD CFX384 system. Samples were run in triplicate. Following and initial denature at 95°C for 5 minutes, then 39 cycles of i) 95°C for 1 minute, ii) annealing at 61°C for 1 minute and then iii) an extension at 72°C for 1 minute. A melting curve analysis was added to determine the quality and specificity of each reaction. Quantification of the PCR reaction was accomplished with iQ Sybr Green Supermix (BIORAD, Hercules, USA). Control samples that omitted DNA resulted in no PCR product. We used PCR Miner (Zhao and Fernald, 2005) to calculate reaction E and CTs. The levels of methylation were calculated as a percent methylation where the levels of enzyme treated DNA are expressed as a percent of untreated enzyme DNA using the following equation: $(1/(1+\text{average enzyme treated DNA efficiency})^{\text{target CT enzyme treated DNA}})/(1/(1+\text{average untreated DNA efficiency})^{\text{target CT untreated DNA}})$ multiplied by 100.

Study 2: In vitro T_4-T_3 conversion by leukocytes—To examine leukocytes $T_4 \rightarrow T_3$ catabolism, lymphocytes were isolated from male hamsters after exposure to either LD (n=8) or SD (n=11) for 10 ± 2 weeks. Physiological responsiveness to SD was confirmed via visual inspection of pelage. Only lymphocytes from hamsters exhibiting fur scores ≥2 (indicative of moult to a winter pelage; Duncan and Goldman, 1984) were collected. At the midpoint of the photocycle (LD: 1030 h; SD: 1400 h; CST), hamsters were anesthetized, and ~1 ml blood was obtained. Blood was diluted in 3 ml sterile RPMI (RPMI 1640; Mediatech, Manassas, VA) and lymphocytes were isolated under sterile conditions via density-gradient centrifugation (Ficoll-Paque PLUS, GE Healthcare). Briefly, diluted blood samples were layered over Ficoll and centrifuged at 400 × *g* for 35 min at 20°C. The lymphocyte layer was extracted and washed twice (500 × *g*, 15 min) with sterile RPMI, and resuspended in RPMI. The concentration and viability of cell suspensions were assessed using Trypan blue exclusion. Samples were adjusted to 5×10^6 lymphocytes/ml, and treated with T_4 within 1 h.

T_4 deiodination assay: Lymphocytes (1×10^6, in 200 ul RPMI) were incubated with 4×10^{-6} M L-thyroxine (T_4; Sigma, T1775) in RPMI for 2 h at 37°C in the dark, according to methods described previously (Smekens et al., 1983). Control samples were incubated with T_4 under identical conditions but contained no lymphocytes. After incubation, cells were immediately frozen at −20°C until assayed. After sonication (3 × 10 s) of the cells in their incubation medium at 0°C, T_3 concentrations were determined in duplicate whole unextracted homogenate samples using a high-sensitivity EIA (MP Biomedicals, Orangeburg, NY). The T_3 EIA had a sensitivity of 0.2 pg/ml, an intra-assay CV of 5.6% and an inter-assay CV of 5.0%. This assay has minimal cross reactivity for T_4 (0.04%).

Study 3: Photoinduced changes in lymphocyte T_3—In order to establish the photoperiodic regulation of cellular localization of T_3 in lymphocytes, male hamsters were housed in LD (n=6) or SD (n=7) for 8 weeks. Reproductive responsiveness to the respective

photoperiods was confirmed 2 days prior to leukocyte collection via measurement of the length and width of the testis under 3% isoflurane anesthesia. Testicular volumes of all hamsters indicated reproductive competence (LD) or gonadal involution (SD). During the later portion of the light phase (5 h prior to lights off), hamsters were anesthetized with isoflurane, and ~1 ml blood was obtained. Lymphocytes were isolated using Ficoll as described above, and 10^6 cells from each animal were fixed with 1.5% paraformaldehyde.

Flow cytometry: Before the experiment, appropriate dilutions of primary and secondary antibodies were established to use saturating antibody concentrations. 10^6 lymphocytes from each sample were permeabilized with icecold 90% methanol (in PBS) at a slow rate while vortexing; after 30 min in methanol on ice, cells were washed 3 × (500 × g, 4°C), and blocked in 500 ul staining buffer for 1 h at 4°C in the dark. Hormone content of permeabilized cells was determined using a primary antibody to T_3 with cross-species reactivity (rabbit anti-T_3; Sigma, T2777; 1:100, 1 h, 4°C, dark; Csaba et al., 2004; Pállinger and Csaba, 2008) followed by detection using FITC-labeled anti-rabbit-FITC-IgG (goat anti-rabbit; Sigma F9887; 1:160, 45 min, 4°C, dark). Cells were then washed 3× and stored at 4°C in darkness until FACS analyses were performed.

Flow cytometry was performed using a CyanADP (DakoCytomation). Negative-controls and single-stained controls were included for use in gating and compensation analyses. All analyses were performed using FlowJo version 8.8.7 (Tree Star Inc., Palo Alto, CA). Lymphocytes were identified based on their forward and side scatter properties, and only single-cells were included in the leukocyte gate. Gates were drawn based on negative stain control samples in which the 1° Ab incubation step was omitted, this allowed discriminating specific from non-specific FITC fluorescence. Cutoffs for negative control staining were always <5% (and typically <1%) of the extreme tail of the distribution of positive-stain controls. All samples were analyzed using the same gates and with the same conditions of voltage on the cytometer. T_3^+ lymphocytes in the lymphocyte/single-cell gate were quantified in terms of proportion (% of parent population) and mean fluorescence intensity (MFI).

Imaging flow cytometry: Cellular localization of T_3 immunofluorescence in lymphocytes from LD (n=6) and SD (n=7) hamsters were single-stained with FITC+ anti-T_3, as described above. Cells were then incubated with nuclear red anthraquinone dye (1:1000, 30 min, 20°C; DRAQ5; eBioscience, San Diego, CA) and visualized on an ImageStream X (ISX) analyzer imaging flow cytometer (Amnis, Seattle, WA), and quantitative image analysis was performed using the Inspire acquisition software. Brightfield, scatter, and fluorescence were captured using a 40× objective. Cells were illuminated with laser lines appropriate for each of the fluorochromes namely, 488 nm for FITC and 658nm for DRAQ5. Laser power was adjusted as necessary to elicit a visible signal without saturating individual pixels. All samples were analyzed using the same gates and with the same conditions of voltage on the ImageStream. This technique has been validated for the detection and subcellular compartmentalization of diverse signaling molecules (e.g., p65, NPAT, IRF-7, Foxo1; George et al., 2006; Maguire et al., 2011; Huang et al., 2012; Rao et al., 2012) in both enriched and mixed cell samples (George et al., 2006). In addition, measurements of nuclear translocation using the Imagestream at 40× magnification are highly positively correlated with measurements of translocation performed using conventional light microscopy (Maguire et al., 2011). A total of 5000 events meeting the classification threshold of a lower limit of Brightfield Area were collected for each sample. The EDF (Extended Depth of Field) optic, along with deconvolution software (built into IDEAS analysis software) was used to resolve punctate staining.

The IDEAS software package (v. 5.0, Amnis) was used for all data analysis. Standard gating strategies to isolate single cells of appropriate size that were well-focused were applied equally to all samples. Briefly, Brightfield Area and Aspect Ratio were use to identify single cell events with expected size ranges, and Brightfield Gradient Root Mean Squared (RMS) was used to exclude cells that fell too far out of the focal plane to garner sufficient quantitative data. A custom nuclear mask based on DRAQ5 staining was derived to measure fluorescence specifically in the nucleus. A compound mask identifying the cellular cytoplasm was derived based on Brightfield area that captured the entire cell minus the nucleus. FITC fluorescence in the nuclear and cytoplasm masks were measured as median fluorescence intensity in order to quantify T_3 in the cellular nucleus and cytoplasm, respectively.

Among the FITC positive fraction, a bimodal distribution was recognized and a region encompassing a FITC high subset was identified. The resulting region was applied equally to all samples, to quantify the number of cells containing high concentrations of immunoreactive T_3 (irT_3). Representative images leukocytes depicting the range of cytoplasmic and nuclear irT_3 levels were gathered from the ISX gallery and exported to a vector graphics program (Adobe Illustrator v. 11.0) for illustrative purposes.

Study 4: Exogenous T_3 effects on blood leukocytes and delayed-time hypersensitivity (DTH) responses—To evaluate whether exogenous T_3 would enhance adaptive immune responses and mimic the SD immunophenotype, male hamsters were housed in LD and received either s.c. saline (0.1 ml) or 1 μg, 5 μg, or 10 μg triiodothyronine (T2877, Sigma Aldrich) (n=15 per group). Another group of hamsters were moved to SD (n=15) and were injected daily with saline. After 3 weeks, whole blood samples were obtained under isoflurane anesthesia, and blood leukocyte concentrations were determined as described above. T_3/saline injections continued, and on week 5, hamsters were sensitized to dinitroflurobenzene (DNFB) on the dorsum and challenged with DNFB on the left ear 7 days later as previously described (Prendergast et al., 2004). Pinna thicknesses were assessed using a constant-load dial micrometer for 7 days post-challenge and are presented as the percent change from baseline (pre-challenge) thickness.

Statistical analyses

For study 1, testes and uteri mass were analyzed using a *t*-test. *dio2*, *dio3*, *dnmt* mRNA and percent *dio3* promoter methylation were analyzed by a 2-way ANOVA. mRNA values were log transformed when a violation of normality was observed. A two-way repeated measures ANOVA was conducted to examine DTH responses. All post-hoc analyses were performed using Fisher's Least Squares Differences unless stated otherwise. Statistical analyses were conducted using SigmaStat 12.0 and differences were considered significant only if $p < 0.05$.

RESULTS

Short days decrease blood leukocyte *dio3* mRNA expression

Siberian hamsters were housed in LD or SD photoperiods. Exposure to SD for 10 weeks resulted in testicular regression (LD: 260±12 mm^3, SD: 45±3 mm^3; t_{21}=14.4, p<0.001; Fig. 1A); vaginal patency was evident in only 30% of SD females, as compared to 100% of LD females (p<0.001; Fig. 1A). Consistent with previous reports (Bilbo et al., 2002; Prendergast et al., 2008), blood leukocyte concentrations were greater in SD relative to LD ($F_{1,40}$=5.11; p<0.05; Fig. 1B).

To examine if leukocytes express iodothyronine deiodinases, RNA was extracted from leukocytes, and *dio2* and *dio3* mRNA expression was measured using qPCR. Photoperiod did not significantly affect leukocyte *dio2* mRNA expression ($F_{1,40}$=0.31; p=0.58; Fig. 1C), but *dio3* expression was markedly inhibited by SD ($F_{1,40}$=10.78; p<0.005; Fig. 1C). These results indicate that circulating leukocytes exhibit the enzymatic capacity to convert T_4 into T_3, and that photoperiod singularly regulates *dio3* expression.

In vitro T_4 to T_3 conversion is enhanced in SD leukocytes

We next examined whether decreases in *dio3* expression in SD leukocytes translate into the predicted disinhibition of T_3 production in SD. Male hamsters were housed in LD or SD, and leukocyte $T_4 \rightarrow T_3$ catabolism was measured by challenging Ficoll-extracted leukocytes with T_4 *in vitro*. T_3 measured in cellular exudate was ~3 fold greater in SD relative to LD leukocytes ($F_{1,13}$=8.90, P<0.01; Fig. 2A, 2B), indicating higher rates of T_4 outer ring deiodination in SD leukocytes.

Short days increase cytoplasmic localization of T_3

To further assess the impact of photoperiod on T_3-signaling in the immune system, the next experiment quantified T_3 expression in blood leukocytes using standard flow cytometric analyses (Fig. 3A, 3B). The proportions of FITC/T_3^+ leukocytes did not differ between LD and SD groups ($F_{1,11}$=0.03, P>0.80; Fig. 3C). Relative (median) fluorescence intensity also did not differ between LD and SD leukocytes ($F_{1,11}$=3.18, P>0.10; Fig. 3D).

The next experiment determined the intracellular localization of T_3. Leukocytes from LD and SD hamsters were extracted from whole blood, fixed, permeablized, and stained with FITC-labeled anti-T_3 antibody along with nuclear red anthraquinone dye (DRAQ5). Cells were visualized on an imaging flow cytometer. An average of 1921 ±1008 (mean ±SD) nucleated cells were identified in each sample (range: 145 – 3416). Consistent with the previous experiment (Fig. 3D), a main effect of photoperiod on T_3 fluorescence intensity was not evident ($F_{1,22}$=0.24, P>0.60, not illustrated); however, brightfield microscopy combined with FITC and DRAQ5 fluorescence identified both nuclear (Fig. 4A) and cytoplasmic (Fig. 4B) localization of T_3 immunofluorescence, and T_3 localization differed as a function of cellular region and photoperiod (photoperiod × region: $F_{1,22}$=16.4, P<0.001). Relative fluorescence intensity was significantly higher in the cytoplasm mask in SD relative to LD leukocytes ($F_{1,11}$=4.97, P<0.05; Fig. 4C), whereas nuclear fluorescence was significantly higher in LD relative to SD leukocytes ($F_{1,11}$=14.3, P<0.005; Fig. 4D). Lastly, the number of lymphocytes expressing high FITC/T_3 fluorescence, independent of intracellular localization, was significantly greater in SD relative to LD hamsters ($F_{1,11}$=6.69, P<0.05; Fig. 4E). Thus, exposure to SD increases the number of circulating lymphocytes that express high levels of intracellular T_3; moreover, in SD T_3 immunofluorescence is preferentially localized in the cytoplasm.

Short days methylate the *dio3* proximal promoter region

We next examined how changes in day length exert transcriptional control of deiodinase mRNA expression. To determine whether epigenetic modifications, in particular DNA methylation, participate in photoperiodic changes in *dio3* expression, DNA methyltransferase (*dnmt*) expression and *dio3* promoter methylation were measured in hamster leukocytes following 10 weeks of adaptation to LD or SD photoperiods. Exposure to SDs did not affect leukocyte *dnmt1* ($F_{1,39}$=0.10; P>0.90) or *dnmt3a* ($F_{1,39}$=0.39; P>0.50) expression, but significantly increased *dnmt3b* mRNA expression ($F_{1,39}$=4.83; P<0.05; Fig. 5A). Because omnibus increases in *dnmt3b* expression in SD lead to increased methylation at multiple DNA residues, we next conducted a methylation-sensitive restriction enzyme (MSRE) assay to quantify the amount of methylated DNA in the *dio3* proximal promoter

per se. MSRE identified greater levels of *dio3* proximal promoter methylation in SD ($F_{1,39}$=8.95; P < 0.005; Fig. 5B).

T_3 treatment mimics effects of SD on immune function *in vivo*

If SD-induced decreases in *dio3* yield local, cell-specific increases in T_3 that participate in photoperiodic changes in immune function, then exogenous T_3 treatment should bypass deiodinase-mediated T_4 catabolism and mimic the effects of SD on immune function, enhancing blood leukocyte numbers and the magnitude of T cell-mediated adaptive skin immune function (as measured via cutaneous DTH responses) (Nelson 2004; Prendergast et al., 2005). Thus, in the next experiment, male hamsters housed in LD were injected with T_3 (1–10 μg) or saline daily for 6 weeks. T_3 increased blood leukocytes in a dose-dependent manner ($F_{4,70}$=6.73; P<0.001; Fig. 6A): 1μg T_3 significantly increased leukocyte concentrations in LD hamsters (P<0.05), and 5μg T_3 yielded leukocyte concentrations indistinguishable from those of SD hamsters (P<0.005 vs. LD).

Antigen-specific skin inflammatory responses (DTH reactions) were also evaluated after 6 weeks of T_3 (1–10 μg, s.c.) treatment. Photoperiod and injection treatments markedly affected DTH reactions ($F_{16,262}$=3.19; P<0.001; Fig. 6B–E). Among saline-treated hamsters, DTH inflammatory responses were significantly greater in SD relative to LD on *days +1* and *+3* after challenge (P<0.05, both comparisons). In LD hamsters treated with 1 μg T_3, only the early (*day +1*) aspects of the DTH reaction were augmented (P<0.05), but T_3 treatments of ≥5 μg were sufficient to mimic the SD-phenotype in the DTH reaction: *day +1* and *+3* pinna thicknesses were significantly greater in these groups relative to saline-treated LD controls (P<0.005, all comparisons). Thus, T_3, in a dose-dependent manner, mimicked the effects of SD on blood leukocyte concentrations and on DTH reactions.

DISCUSSION

Seasonally-changing immunophenotypes are ubiquitous in nature and evident across diverse vertebrate taxa (Nelson, 2004; Nelson and Demas, 1996); changes in the host response to antigen challenge or infection likely contributes to seasonal rhythms in morbidity and mortality. Changes in environmental photoperiod drive seasonal plasticity in immune function (Nelson and Demas, 1996), and here we report a novel mechanism by which changes in photoperiod impose these distinct seasonal immunophenotypes. T_4 to T_3 conversion, a key pathway by which photoperiod regulates reproductive function in the CNS, also plays a central role in the transmission of seasonal time information into the immune system. Central to this mechanism is a robust inhibitory effect of SD photoperiods on *dio3* mRNA expression at the level of the leukocyte. Decreases in *dio3* mRNA expression reduce the conversion of the prohormone, T_4, into rT_3. Against a background of photoperiod-invariant *dio2* expression (Fig. 1), a lower *dio2*:*dio3* ratio favors the production of T_3, and increases in T_3 signaling enhance constitutive and adaptive immunity. Indeed, functional *in vitro* assays confirmed that the hormonal microenvironment in blood lymphocytes in SD favors T_3 production. The data also indicate that photoperiod exerts these effects on *dio3* mRNA expression via epigenetic mechanisms: adaptation to SD increases *dnmt3b* expression, which increases the methylation status of the *dio3* proximal promoter and inhibits *dio3* expression. The present work demonstrates that elevated T_3 in SD leukocytes is primarily localized in the cytoplasm, consistent with extranuclear mediation of T_3-enhancement of multiple aspects of immune function (Mascanfroni et al., 2008, 2010). Lastly, as predicted by this model, T_3 treatments were sufficient to mimic the effects of SD on several diagnostic measures of immunity in LD-housed hamsters. Together, the data suggest that photoperiodic modulation of DNA methylation in a single gene (*dio3*)

promoter region may be a key mechanism by which day length engages changes in T_3 signaling in lymphoid cells and drives seasonal plasticity in immune function.

Epigenetic regulation of triiodothyronine signaling governs seasonal immunological plasticity

The local conversion of T_4 into T_3 in the brain is essential for the photoperiodic regulation of seasonal reproduction (Yoshimura et al., 2003). In birds and mammals (Nakao et al., 2008; Hanon et al., 2008; Barrett et al., 2007; Ono et al., 2008; Prendergast et al., 2013b), hypothalamic levels of *dio2* and/or *dio3* expression act as a molecular switch that governs the local availability of T_3. Here we show that blood leukocytes express both *dio2* and *dio3* mRNA, and that *dio3* exhibits marked photoperiodic variation, with greater levels of expression in LD hamsters. Note that, following photoperiod manipulations, the direction of change in *dio3* expression in leukocytes is the opposite of that which occurs in the hypothalamus [cf. Prendergast et al., 2013b]; thus, decreased *dio3* expression in SD leukocytes would be predicted to amplify the T_3 signal in leukocytes, at a time of year when T_3 signaling is attenuated in the CNS. Such a mechanism would be poised to control immunity and mediate effects of day length on the immune system at a cell-specific level.

Epigenetic mechanisms likely participate in the photoperiodic regulation of *dio3* mRNA expression. DNA methyltransferases (DNMTs) mediate methylation of CpG residues at multiple stages of development (Reik et al., 2001; Smith and Meissner, 2013). Noteworthy in the present study is the robust upregulation of leukocyte *dnmt3b* mRNA expression following adaptation to SD. Elevated *dnmt3b* expression would be expected to promote high levels of CpG methylation (Jones and Liang, 2009). Presumably, such increases in DNA methylation could occur across the entire genome; however, a methylation assay specific to the *dio3* proximal promoter (Fig. 5B) indicated a ~50% increase in methylation in SD, suggesting that *dio3* is a likely target of DNMT3b enzymatic activity, although it is unlikely to be the only target. Additional, convergent, evidence will be required to establish the specific DNA motifs that are methylated following adaptation to SD; the presence of higher levels of DNMT3b (or MeCP2) in the *dio3* promoter in SD would constitute direct evidence in this regard, and current investigations employing chromatin immunoprecipitation assays may permit resolution of this issue.

Cell-autonomous catabolism of T_3 in peripheral leukocytes

Photoperiod also altered the ability of leukocytes to catabolize T_4 into T_3. In Siberian hamsters, circulating T_4 and T_3 concentrations do not respond to changes in photoperiod (O'Jile and Bartness, 1992). Thus, against a background of seasonally-invariant prohormone (T_4) and *dio2* expression, decreased *dio3* mRNA expression in SD leukocytes would be predicted to favor the conversion of T_4 to T_3. Indeed, T_3 production was significantly (~3 fold) greater in SD relative to LD lymphocytes (Fig. 2). Although the present data do not permit the conclusion that decreases in *dio3* mRNA in SD leukocytes are responsible for enhanced *in vitro* T_3 catabolism in SD cells, this outcome is consistent with what would be predicted if SD-induced decreases in *dio3* expression were functional at a cellular level *in vivo*: driving the T_4 catabolic pathway away from rT_3 production and towards increased T_3 production, resulting in greater T_3 signaling in SD relative to LD lymphocytes. Greater *dio3* mRNA in LD likely increases rT_3 production as well. One limitation of the present work is that lymphocyte production of rT_3, and immunological responses to rT_3 were not examined. However, few metabolic effects of rT_3 have been reported in the literature, and a role, if any, for rT_3 in mediating seasonal changes in immunity is currently unknown.

To further characterize photoperiodic effects on lymphoid T_3 signaling, follow-up experiments examined the number of leukocytes containing immunoreactive T_3, and the

cellular localization of T_3 via imaging flow cytometry. Although the overall proportion of T_3^+ lymphocytes did not vary across photoperiod, the number of lymphocytes expressing high intracellular T_3 was significantly greater in SD relative to LD hamsters. Importantly, T_3 fluorescence intensity differed markedly as a function of cellular region: T_3 fluorescence was higher in the cytoplasm in SD, whereas T_3 was higher in the nucleus LD. Thus, the net effect of adaptation to SD is an increase in the number of leukocytes with high concentrations of intracellular T_3, and enhancing cytoplasmic T_3 localization. In human and rhesus macaque cells, DIO3 enzymes are localized in the plasma membrane, where it functions to decrease local T_4 and T_3 concentrations, preventing access of active T_3 to the cytoplasm (Baqui et al., 2003). If DIO3 is similarly localized in Siberian hamster lymphocytes, then it would be well-positioned to rapidly decrease cytoplasmic T_3 in LD.

Until relatively recently, T_3 effects were presumed to be mediated via T_3 binding to nuclear thyroid hormone receptors (TRs); however, numerous recent reports indicate extranuclear effects of TR mediated T_3 signaling in the control of, e.g., angiogenesis (Baumann et al,. 2001) and lymphocyte maturation (Mascanfroni et al., 2008), and it is now well-established that TRs may shuttle rapidly between the nuclear and cytosolic compartments (Baumann et al., 2001; Hager et al., 2000). Indeed, T_3-signaling through TRβ1 in the cytoplasm is an essential step in the maturation of dendritic cells (Mascanfroni et al., 2008), which play a critical role in antigen presentation during the DTH response (Sadhu et al., 2007). Together, the present data suggest that exposure to short photoperiods increase lymphocyte T_3 production and increases the number of T_3-containing lymphocytes in the circulation. SD photoperiods also inhibit nuclear, and increase cytosolic T_3 localization (Fig. 3). A limitation of the current study is that the experiments did not identify the lymphocyte phenotypes that exhibited increases in T_3 in SD. Previous reports indicate that SD photoperiods increase the number of circulating T cells, which participate in immunological memory-dependent adaptive immune responses (Bilbo et al., 2002). Increases in intracellular T_3 signaling in T cells may augment T cell-dependent inflammatory responses (cf. *Experiment 4*). In light of recent work indicating a cytoplasmic role for TR-signaling in the differentiation and maturation of some leukocyte subtypes (e.g., antigen presenting cells; APCs), and given the critical role of activated APCs in the formation of immunological memory (Varona et al., 2001) and in antigen-specific inflammatory responses (Sadhu et al, 2007), enhanced cytoplasmic T_3 signaling under SD is consistent with the immunological plasticity observed following adaptation to SD photoperiods (e.g., increases in blood leukocyte concentrations and enhanced DTH reactions).

Experiment 1 identified deiodinase mRNA responses to photoperiod in the entire blood leukocyte population, whereas Experiments 2 and 3 assessed T_3 production and immunoreactivity in the lymphocyte subset of blood leukocytes. Photoperiodic effects on lymphocyte T_4 deiodination and T_3 cellular compartmentalization were evident in the lymphocyte subset, suggesting that either: (1) photoperiodic changes in *dnmt* and *dio3* expression may be occurring across many subpopulations of leukocytes, or (2) photoperiodic changes in these genes may be occurring only in the lymphocyte subpopulation. The present data do not permit discrimination among these hypotheses. If the former hypothesis were true, it would suggest that photoperiod effects on leukocyte biology are pervasive; whereas if the latter hypothesis were true, it would imply that whole blood leukocyte measures, considerably diluted by non-lymphocytes, may be underestimating the photoperiodic induction of *dio3*.

Thyroid enhancement of immunity

To test the biological significance of SD-induced increases in cellular $T_4 \rightarrow T_3$ conversion, two final experiments bypassed the relatively low endogenous T_3 biosynthesis in LD

leukocytes by administering T_3 to hamsters housed in LD for seasonal time intervals (6 weeks). Exogenous T_3 mimicked the effects of SD photoperiods on multiple aspects of immune function, consistent with the aforementioned model in which increases in cell-specific T_3 signaling mediate SD-induced enhancements in immune function. In prior work in rats, pharmacological doses of T_4 or T_3 enhanced select measures of immunity including blastogenic responses to antigens *in vitro* and DTH inflammatory responses (Chandel and Chatterjee, 1989; Chatterjee and Chandel, 1983). The present work suggests that such observations may have inadvertently been mimicking the enhanced T_3 signaling under SD photoperiods; however, it is unclear why in such studies, T_4 treatments were as effective as T_3 treatments, absent any manipulations of photoperiod. In the present report, it is likely that some conversion of exogenous T_3 into T_2 (by *dio3*) may be occurring in LD lymphocytes. Such a process might explain why lower doses of T_3 (1 μg) were less effective than higher doses (5 and 10 μg) in enhancing aspects of immunity. However, at higher doses of T_3, such enzymatic activity is unlikely to be able to fully catabolize T_3 into T_2.

The present data clearly identify a dose-response relationship between T_3 treatment and trait-specific immunoenhancement. Blood leukocyte concentrations were enhanced in a dose-dependent manner, with an inverted U-shape function and a response maximum mimicking the effects of SD at 5 μg (~125 μg/kg). Furthermore, although the present work did not identify leukocyte subpopulations, prior work has established that SD-augmentation of blood leukocyte concentrations are primarily mediated by increases in T-cells and NK cells, but not B-cells, monocytes, or neutrophils (Bilbo et al., 2002; Prendergast et al., 2004; Prendergast et al., 2008). It was not determined if the proportions of T_3+ lymphocytes changed following T_3 treatment.

The DTH results are likewise consistent with augmented T cell activity, and DTH was enhanced by T_3 treatments, the effects of which either peaked or reached an asymptote at the 5 μg treatment dose. Enhanced T_3 signaling, either mediated via photoperiod-induced changes in *dio3* expression or via exogenous treatment, may augment DTH reactions via multiple, non-exclusive mechanisms: either (1) via enhancing T cell interactions with APCs or (2) via facilitating maturation of dendritic cells. Substantial evidence suggests that T_3–induced dendritic cell maturation facilitates naïve T cell proliferation and IFN-γ production (Mascanfroni et al., 2008); T_3 also plays a key role in the cytoplasmic-nuclear shuttling of nuclear factor κβ on primed dendritic cells (Mascanfroni et al., 2010). Increased cytoplasmic T_3 in SD leukocytes, together with enhanced DTH reactions in SD (or following T_3 treatment in LD), provide convergent evidence in support of a role of cell-specific T_3 signaling in the induction of seasonal immunophenotypes.

CONCLUSIONS

The proximate causes of numerous human rhythms in health and immune function remain largely unknown. Understanding the mechanisms by which time information induces these changes in immune function stands to identify novel endogenous mechanisms by which the neuroendocrine system and the immune system interact. The present data describe a novel mechanism by which environmental day length cues gain access to the immune system: changes in photoperiod alter T_3-signaling in lymphoid cells via epigenetic transcriptional regulation of *dio3*. It is worth noting that photoperiodic changes in immune function are evident in reproductively non-photoperiodic species (Prendergast et al., 2007, Gatien et al., 2004), thus, the mechanism described here may have relevance beyond seasonally-breeding rodents. Indeed, photoperiod-driven changes in hypothalamic *dio2* and *dio3* expression persist in mice and rats, despite the absence of photoperiodic gonadotropin responses (Ross et al., 2011; Ono et al., 2008). Noteworthy also is that direction of the effect of SD on leukocyte T_3 signaling is the exact opposite of that induced by SD in the reproductive

neuroendocrine system (Nakao et al., 2008; Hanon et al., 2008; Barrett et al., 2007; Ono et al., 2008; Prendergast et al., 2013b). Whereas the outcome of Experiment 4 permits strong inferences on the sufficiency of T_3, the necessity of T_3 signaling in this regard remains to be established. Experiments 1–3 provide convergent evidence suggest that leukocyte *dio3* expression orchestrates these endocrine effects on immune function. Additional experiments, in which *dio3* expression is selectively enhanced or suppressed, will be required to examine the necessity and sufficiency of photoperiodic changes in *dio3* mRNA in the mediation of seasonal changes in immunity. Cell-autonomous regulation of *dio3* expression by photoperiod may afford tissue-specific flexibility in the direction of change in thyroid hormone signaling in order to allow seasonally-appropriate changes in reproductive and immune function to occur concurrently in response to a common photoperiod cue. Taken together, the data suggest a novel mechanism by which time information impacts the immune system.

Supplementary Material

Refer to Web version on PubMed Central for supplementary material.

Acknowledgments

The authors thank Drs. Betty Theriault and Priyesh Patel for expert technical assistance, and the University of Chicago Comprehensive Cancer Center DNA Sequencing and Genotyping Facility for sequencing instrumentation and expertise. This work was funded by grant NIH NIAID AI-67406 and by NIH grant UL1 TR000430 from the National Center for Advancing Translational Sciences.

REFERENCES

Arpin C, Pihlgren M, Fraichard A, Aubert D, Samarut J, Chassande O, Marvel J. Effects of T3R alpha 1 and T3R alpha 2 gene deletion on T and B leukocyte development. J. Immunol. 2000; 164:152–160. [PubMed: 10605006]

Baqui M, Botero D, Gereben B, Curcio C, Harney JW, Salvatore D, Sorimachi K, Larsen PR, Bianco AC. Human Type 3 iodothyronine selenodeiodinase is located in the plasma membrane and undergoes rapid internalization to endosomes. J Biol. Chem. 2003; 278:1206–1211. [PubMed: 12419801]

Barrett P, Ebling FJ, Schuhler S, Wilson D, Ross AW, Warner A, Jethwa P, Boelen A, Visser TJ, Ozanne DM, Archer ZA, Mercer JG, Morgan PJ. Hypothalamic thyroid hormone catabolism acts as a gatekeeper for the seasonal control of body weight and reproduction. Endocrinology. 2007; 148:3608–3617. [PubMed: 17478556]

Baumann CT, Maruvada P, Hager GL, Yen PM. Nuclear cytoplasmic shuttling by thyroid hormone receptors. multiple protein interactions are required for nuclear retention. J. Biol. Chem. 2001; 276:11237–11245. [PubMed: 11152480]

Bechtold DA, Gibbs JE, Loudon AS. Circadian dysfunction in disease. Trends Pharmacol. Sci. 2010; 31:191–198. [PubMed: 20171747]

Bergh JJ, Lin HY, Lansing L, Mohamed SN, Davis FB, Mousa S, Davis PJ. Integrin alphaVbeta3 contains a cell surface receptor site for thyroid hormone that is linked to activation of mitogen-activated protein kinase and induction of angiogenesis. Endocrinology. 2005; 146:2864–2871. [PubMed: 15802494]

Bianco AC, Salvatore D, Gereben B, Berry MJ, Larsen PR. Biochemistry, cellular and molecular biology, and physiological roles of the iodothyronine selenodeiodinases. Endocrine Rev. 2002; 23:38–89. [PubMed: 11844744]

Bilbo SD, Dhabhar FS, Viswanathan K, Saul A, Yellon SM, Nelson RJ. Short day lengths augment stress-induced leukocyte trafficking and stress induced enhancement of skin immune function. Proc. Natl. Acad. Sci. USA. 2002; 99:4067–4072. [PubMed: 11904451]

Chandel AS, Chatterjee S. Effect of thyroid hormones on delayed type hypersensitivity reaction. Indian J. Exp. Biol. 1989; 27:408–411. [PubMed: 2599550]

Chatterjee S, Chandel AS. Immunomodulatory role of thyroid hormones: in vivo effect of thyroid hormones on the blastogenic response of lymphoid tissues. Acta Endocrinol. 1983; 103:95–100. [PubMed: 6602446]

Csaba G, Kovács P, Pállinger E. Immunologically demonstrable hormones and hormone-like molecules in rat white blood cells and mast cells. Cell Biol. Int. 2004; 28:487–490. [PubMed: 15223027]

Dorshkind K, Horseman ND. The roles of prolactin, growth hormone, insulin-like growth factor-I and thyroid hormone in leukocyte development and function: insights from genetic models of hormone and hormone receptor deficiency. Endocr. Rev. 2000; 21:292–312. [PubMed: 10857555]

Duncan MJ, Goldman MD. Hormonal regulation of the annual pelage color cycle in the Djungarian hamster, Phodopus sungorus. I. role of the gonads and pituitary. J. Exp. Zool. 1984; 230:89–95. [PubMed: 6726149]

Foster MP, Jensen ER, Montecino-Rodriguez E, Leathers H, Horseman N, Dorshkind K. Humoral and cell-mediated immunity in mice with genetic deficiencies of prolactin, growth hormone, insulin like growth factor-I, and thyroid hormone. Clin. Immunol. 2000; 96:140–149. [PubMed: 10900161]

Foster MP, Montecino-Rodriguez E, Dorshkind K. Proliferation of bone marrow pro-B cells is dependent on stimulation by the pituitary/thyroid axis. J. Immunol. 1999; 163:5883–5890. [PubMed: 10570273]

Freeman DA, Kampf-Lassin A, Galang J, Wen JC, Prendergast BJ. Melatonin acts at the suprachiasmatic nucleus to attenuate behavioral symptoms of infection. Behav. Neurosci. 2007; 121:689–697. [PubMed: 17663594]

Gatien ML, Hotchkiss AK, Neigh GN, Dhabhar FS, Nelson RJ. Immune and stress responses in C57BL/6 and C3H/H3N mouse strains following photoperiod manipulation. Neuro Endocrinol. Lett. 2004; 25:267–272. [PubMed: 15361815]

George TC, Fanning SL, Fitzgerald-Bocarsly P, Medeiros RB, Highfill S, Shimizu Y, Hall BE, Frost K, Basiji D, Ortyn WE, Morrissey PJ, Lynch DH. Quantitative measurement of nuclear translocation events using similarity analysis of multispectral cellular images obtained in flow. J. Immunol. Methods. 2006; 311:117–129. [PubMed: 16563425]

Hager GL, Lim CS, Elbi C, Baumann CT. Trafficking of nuclear receptors in living cells. J. Steroid Biochem. Mol. Biol. 2000; 74:249–254. [PubMed: 11162932]

Hanon EA, Lincoln GA, Fustin JM, Dardente H, Masson-Pevet M, Morgan PJ, Hazlerigg DG. Ancestral TSH mechanism signals summer in a photoperiodic mammal. Curr. Biol. 2008; 18:1147–1152. [PubMed: 18674911]

Huang YH, Sojka DK, Fowell DJ. Cutting edge: Regulatory T cells selectively attenuate, not terminate, T cell signaling by disrupting NF-κB nuclear accumulation in CD4 T cells. J. Immunol. 2012; 188:947–951. [PubMed: 22227565]

Jones PA, Liang G. Rethinking how DNA methylation patterns are maintained. Nat. Rev. Genet. 2009; 12:805–811. [PubMed: 19789556]

Logan RW, Sarkar DK. Circadian nature of immune function. Mol. Cell. Endocrinol. 2012; 349:82–90. [PubMed: 21784128]

Maguire O, Collins C, O'Loughlin K, Miecznikowski J, Minderman H. Quantifying nuclear p65 as a parameter for NF-κB activation: Correlation between ImageStream cytometry, microscopy, and Western blot. Cytometry A. 2011; 79:461–469. [PubMed: 21520400]

Mascanfroni ID, Montesinos MM, Alamino VA, Susperreguy S, Nicola JP, Ilarregui JM, Masini-Repiso AM, Rabinovich GA, Pellizas CG. Nuclear factor (NF)-kappaB-dependent thyroid hormone receptor beta1 expression controls dendritic cell function via Akt signaling. J. Biol. Chem. 2010; 285:9569–9582. [PubMed: 20018842]

Mascanfroni ID, Montesinos MM, Susperreguy S, Cervi L, Ilarregui JM, Ramseyer VD, Masini-Repiso AM, Targovnik HM, Rabinovich GA, Pellizas CG. Control of dendritic cell maturation and function by triiodothyronine. FASEB J. 2008; 22:1032–1042. [PubMed: 17991732]

Montecino-Rodriguez E, Clark R, Johnson A, Collins L, Dorshkind K. Defective B cell development in Snell dwarf (dw/dw) mice can be corrected by thyroxine treatment. J. Immunol. 1996; 157:3334–3340. [PubMed: 8871629]

Murphy WJ, Durum SK, Anver MR, Longo DL. Immunologic and hematologic effects of neuroendocrine hormones. Studies on DW/J dwarf mice. J. Immunol. 1992; 148:3799–3805. [PubMed: 1602129]

Nakao N, Ono H, Yamamura T, Anraku T, Takagi T, Higashi K, Yasuo S, Katou Y, Kageyama S, Uno Y, Kasukawa T, Iigo M, Sharp PJ, Iwasawa A, Suzuki Y, Sugano S, Niimi T, Mizutani M, Namikawa T, Ebihara S, Ueda HR, Yoshimura T. Thyrotrophin in the pars tuberalis triggers photoperiodic responses. Nature. 2008; 452:317–322. [PubMed: 18354476]

Nelson RJ. Seasonal immune function and sickness responses. Trends Immunol. 2004; 25:187–192. [PubMed: 15039045]

Nelson RJ, Demas GE. Seasonal changes in immune function. Q. Rev. Biol. 1996; 71:511–548. [PubMed: 8987173]

O'Jile JR, Bartness TJ. Effects of thyroxine on the photoperiodic control of energy balance and reproductive status in Siberian hamsters. Physiol. Behav. 1992; 52:267–270. [PubMed: 1523252]

Ono H, Hoshino Y, Yasuo S, Watanabe M, Nakane Y, Murai A, Ebihara S, Korf HW, Yoshimura T. Involvement of thyrotropin in photoperiodic signal transduction in mice. Proc. Natl. Acad. Sci. USA. 2008; 105:18238–18242. [PubMed: 19015516]

Pállinger E, Csaba G. A hormone map of human immune cells showing the presence of adrenocorticotropic hormone, triiodothyronine and endorphin in immunophenotyped white blood cells. Immunology. 2008; 123:584–589. [PubMed: 18005034]

Prendergast BJ, Baillie SR, Dhabhar FS. Gonadal hormone-dependent and -independent regulation of immune function by photoperiod in Siberian hamsters. Am. J. Physiol. Regul. Integr. Comp. Physiol. 2008; 294:R384–R392. [PubMed: 17989142]

Prendergast BJ, Bilbo SD, Dhabhar FS, Nelson RJ. Effects of photoperiod history on immune responses to intermediate day lengths in Siberian hamsters (*Phodopus sungorus*). J. Neuroimmunol. 2004; 149:31–39. [PubMed: 15020062]

Prendergast BJ, Bilbo SD, Nelson RJ. Short day lengths enhance skin immune responses in gonadectomised Siberian hamsters. J. Neuroendocrinol. 2005; 17:18–21. [PubMed: 15720471]

Prendergast BJ, Hotchkiss AK, Nelson RJ. Photoperiodic regulation of circulating leukocytes in juvenile Siberian hamsters: mediation by melatonin and testosterone. J. Biol. Rhythms. 2003; 18:473–480. [PubMed: 14667148]

Prendergast BJ, Kampf-Lassin A, Yee JR, Galang J, McMaster N, Kay LM. Winter day lengths enhance T lymphocyte phenotypes, inhibit cytokine responses, and attenuate behavioral symptoms of infection in laboratory rats. Brain Behav. Immun. 2007; 21:1096–1108. [PubMed: 17728099]

Prendergast BJ, Pyter LM, Kampf-Lassin A, Patel PN, Stevenson TJ. Rapid induction of hypothalamic iodothyronines deiodinase expression by photoperiod and melatonin in juvenile Siberian hamsters. Endocrinology. 2013a; 154:831–841. [PubMed: 23295738]

Prendergast BJ, Cable EJ, Patel PN, Pyter LM, Onishi KJ, Stevenson TJ, Ruby NF, Bradley SP. Impaired leukocyte trafficking and skin inflammatory responses in hamsters lacking a functional circadian system. Brain Behav. Immun. 2013b; 32:94–104. [PubMed: 23474187]

Prendergast, BJ.; Zucker, I.; Nelson, RJ. Seasonal rhythms of mammalian behavioral neuroendocrinology. In: Pfaff, D.; Arnold, A.; Etgen, A.; Fahrbach, S.; Moss, R.; Rubin, R., editors. Hormones, Brain, and Behavior. 2nd edition. San Diego: Academic Press; 2009. p. 507-538.

Rao RR, Li Q, Bupp MRG, Shrikant PA. Transcription factor foxo1 represses T-bet-mediated effector functions and promotes memory CD8+ T cell differentiation. Immunity. 2012; 36:374–387. [PubMed: 22425248]

Reik W, Dean W, Walter J. Epigenetic reprogramming in mammalian development. Science. 2001; 293:1089–1093. [PubMed: 11498579]

Ross AW, Helfer G, Russell L, Darras VM, Morgan PJ. Thyroid hormone signaling genes are regulated by photoperiod in the hypothalamus of F344 rats. PLoS One. 2011; 6:e21351. [PubMed: 21731713]

Sadhu C, Ting HJ, Lipsky B, Hensley K, Garcia-Martinez LF, Simon SI, Staunton DE. CD11c/CD18: novel ligands and a role in delayed-type hypersensitivity. J. Leukoc. Biol. 2007; 81:1395–1403. [PubMed: 17389580]

Segal J, Ingbar SH. Specific binding sites for the triiodothyronine in the plasma membrane of rat thymocytes. Correlation with biochemical responses. J. Clin. Invest. 1982; 70:919–926. [PubMed: 6290538]

Smekens L, Golstein J, Vanhaelst L. Measurement of thyroxine conversion to triiodothyronine using human lymphocytes. A useful and simple laboratory technique. J. Endocrinol. Invest. 1983; 6:113–117. [PubMed: 6863848]

Smith ZD, Meissner A. DNA methylation: roles in mammalian development. Nat. Rev. Genet. 2013; 14:204–220. [PubMed: 23400093]

St Germain DL, Galton VA, Hernandez A. Minireview: defining the roles of the iodothyronine deiodinases: current concepts and challenges. Endocrinology. 2009; 150:1097–1107. [PubMed: 19179439]

Varona R, Villares R, Carramolino L, Goya I, Zaballos A, Gutierrez J, Torres M, Martinez-A C, Marquez G. CCR6-deficient mice have impaired leukocyte homeostasis and altered contact hypersensitivity and delayed-type hypersensitivity responses. J. Clin. Invest. 2001; 107:R37–R45. [PubMed: 11254677]

Walton JC, Weil ZM, Nelson RJ. Influence of photoperiod on hormones, behavior and immune function. Front. Neuroendocrinol. 2011; 32:303–319. [PubMed: 21156187]

Wen JC, Dhabhar FS, Prendergast BJ. Pineal-dependent and -independent effects of photoperiod on immune function in Siberian hamsters (*Phodopus sungorus*). Horm. Behav. 2007; 51:31–39. [PubMed: 17022983]

Yamamura T, Hirunagi K, Ebihara S, Yoshimura T. Seasonal morphological changes in the neuro-glial interaction between gonadotropin-releasing hormone nerve terminals and glial endfeet in Japanese quail. Endocrinology. 2004; 145:4264–4267. [PubMed: 15178649]

Yasuo S, Yoshimura T. Comparative analysis of the molecular basis of photoperiodic signal transduction in vertebrates. Integr. Comp. Biol. 2009; 49:507–518. [PubMed: 21665837]

Yellon SM, Teasley LA, Fagoaga OR, Nguyen HC, Truong HN, Nehlsen-Cannarella L. Role of photoperiod and the pineal gland in T cell-dependent humoral immune reactivity in the Siberian hamster. J. Pineal Res. 1999; 27:243–248. [PubMed: 10551773]

Yoshimura T, Yasuo S, Watanabe M, Iigo M, Yamamura T, Hirunagi K, Ebihara S. Light-induced hormone conversion of T_4 to T_3 regulates photoperiodic responses of gonads in birds. Nature. 2003; 426:178–181. [PubMed: 14614506]

Zhao S, Fernald RD. Comprehensive algorithm for quantitative real-time polymerase chain reaction. J. Comput. Biol. 2005; 12:1047–1064. [PubMed: 16241897]

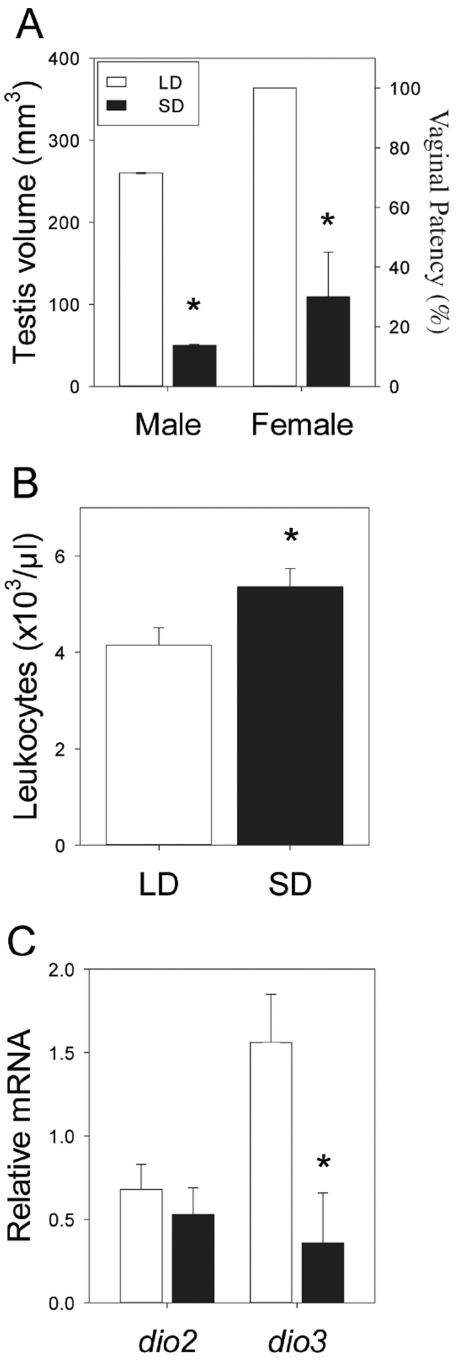

Figure 1. Short days increase blood leukocyte concentrations and inhibit *dio3* expression

(A) Testis volumes of males (left) and percentage of females with patent vaginae (right) following 10 weeks of exposure to long (15L:9D; LD) or short (9L:15D; SD) photoperiods. (B) Blood leukocyte concentrations. (C) Blood leukocyte *dio2* (left) and *dio3* (right) mRNA expression. Data are mean +SEM, * P<0.05 vs. LD value.

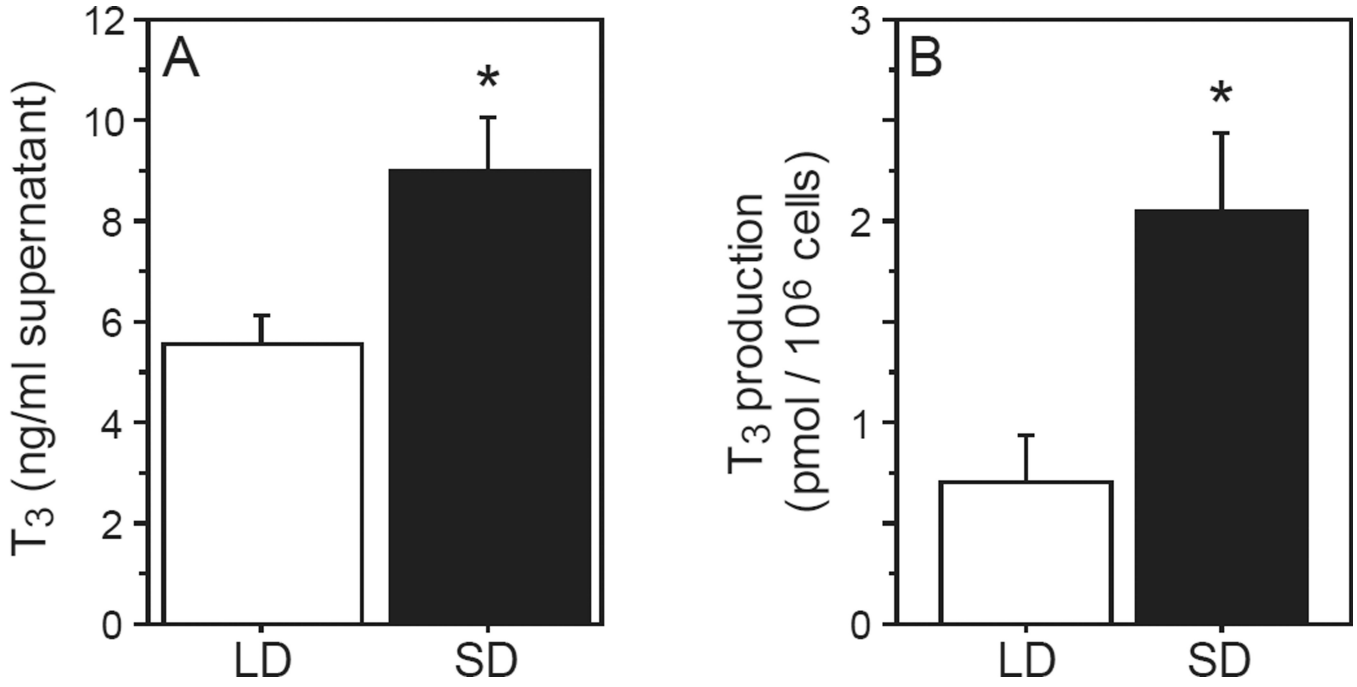

Figure 2. Short days increase *in vitro* T_4 catabolism

Mean +SEM (A) supernatant T_3 concentrations and (B) T_3 production (expressed as pmol/10^6 lymphocytes) of Ficoll-extracted blood lymphocytes obtained from adult Siberian hamsters after 10 weeks of exposure to LD or SD photoperiods. Lymphocytes were incubated *in vitro* with T_4 (4×10^{-6} M) for 2 h prior to T_3 determinations. *P<0.01 vs. LD value.

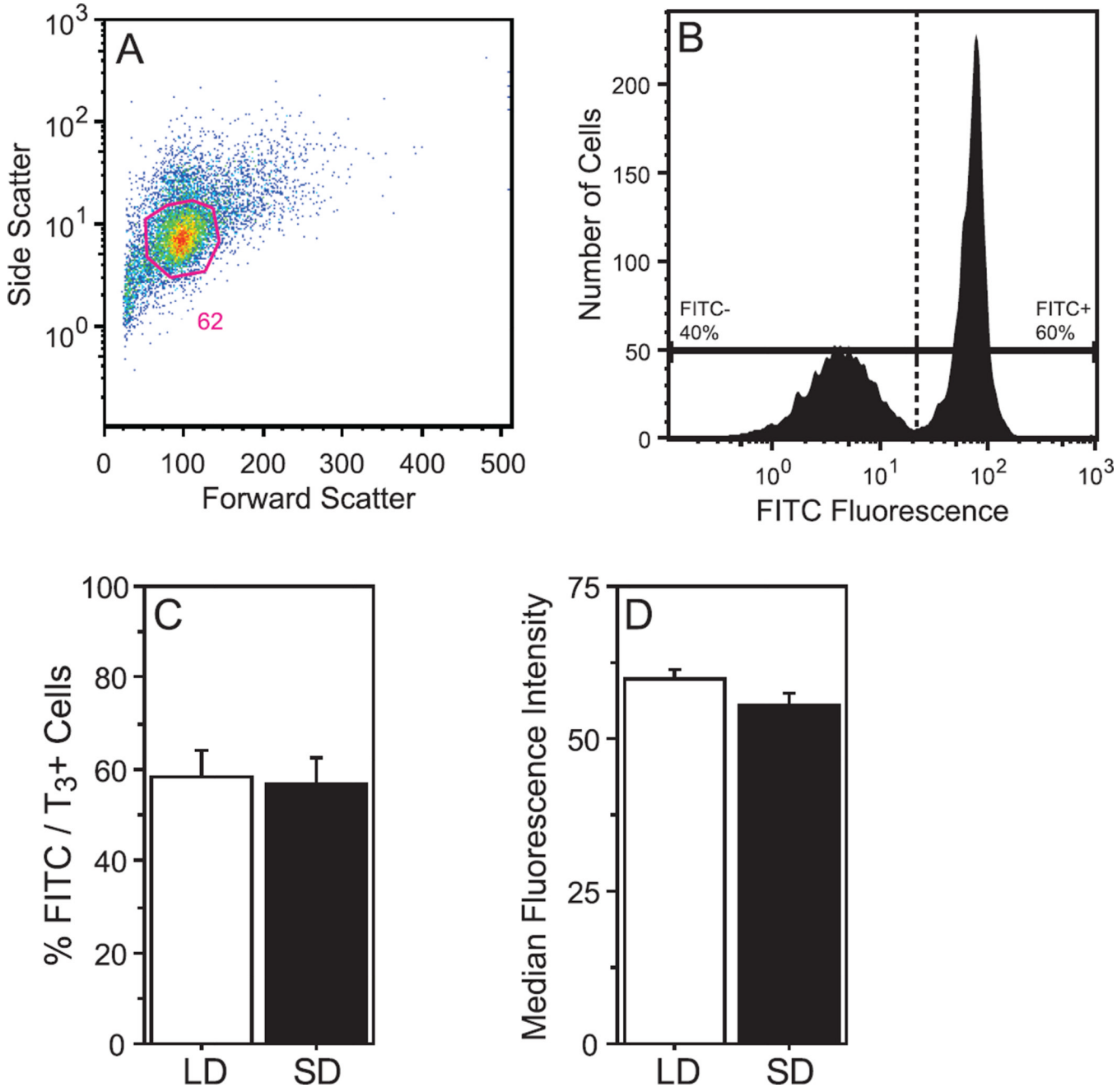

Figure 3. Photoperiod does not affect the overall proportion of T_3^+ lymphocytes in blood

(A) Representative dot plots demonstrating the method of gating (FSC, forward scatter; SSC, side scatter) for lymphocytes. (B) Representative histogram depicting gating strategy for specific (FITC+) and non-specific (FITC−) T_3 immunofluorescence. Identical gates were applied to all samples. Mean +SEM (C) percentage of FITC/T_3^+ events, and (D) median fluorescence intensity of FITC/T_3^+ events.

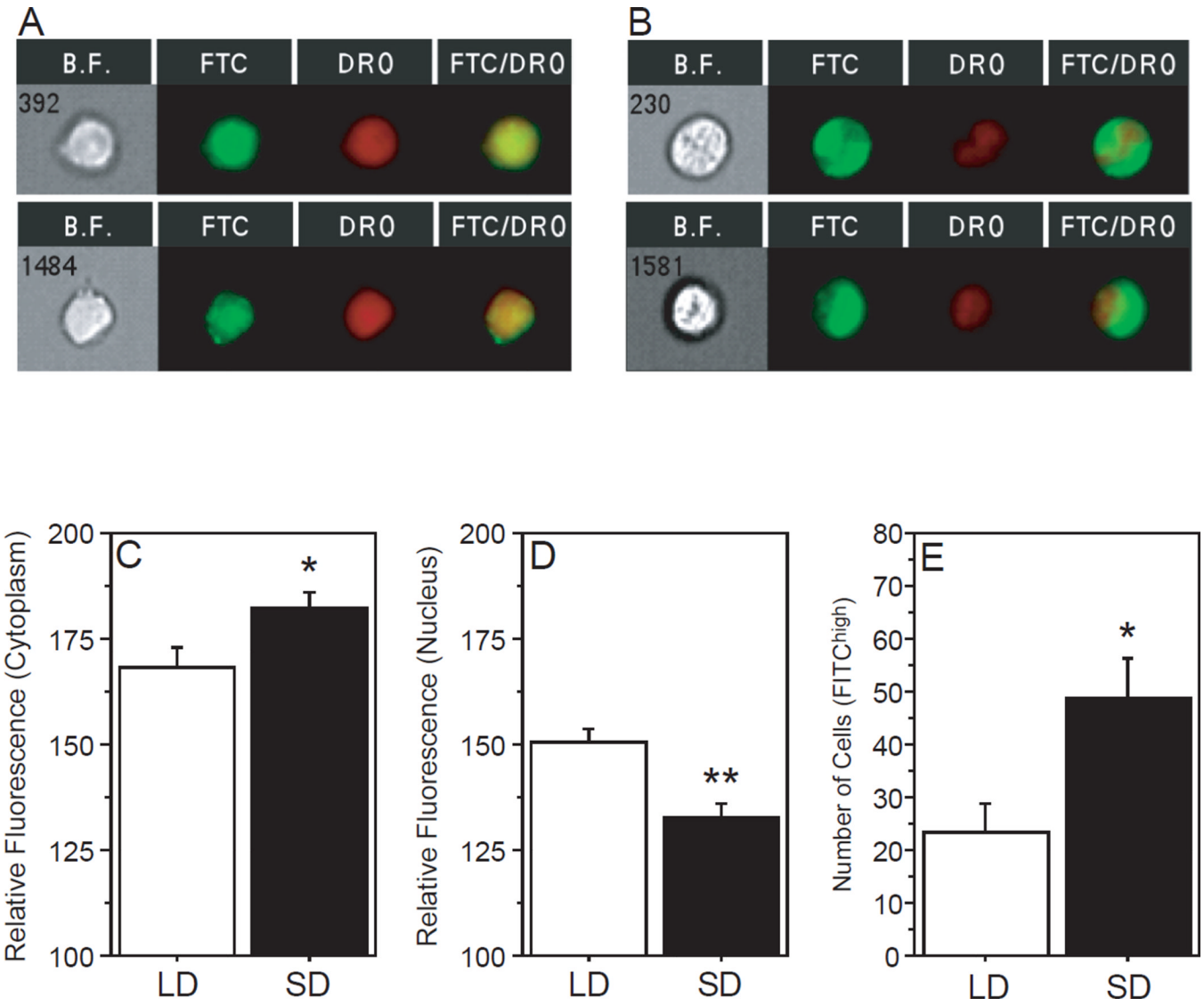

Figure 4. Photoperiod alters intracellular localization of T_3 in blood lymphocytes

Representative images of T_3^+/DRAQ5$^+$ fluorescence obtained at 40× magnification on the ImageStreamX imaging flow cytometer (BF= brightfield image, FTC= FITC/T_3^+ channel, DRQ= nuclear DRAQ5$^+$ channel, FTC/DRQ= overlay) of Ficoll-extracted blood lymphocytes obtained from Siberian hamsters after 10 weeks of exposure to LD or SD photoperiods. Relative FITC/T_3^+ fluorescence in the (C) cytoplasmic and (D) nuclear cellular regions as identified by DRAQ5$^-$ and DRAQ5$^+$ overlap, respectively. (E) Number of FITC/T_3^{high} lymphocytes, independent of intracellular localization. *P<0.05, **P<0.005 vs. LD value.

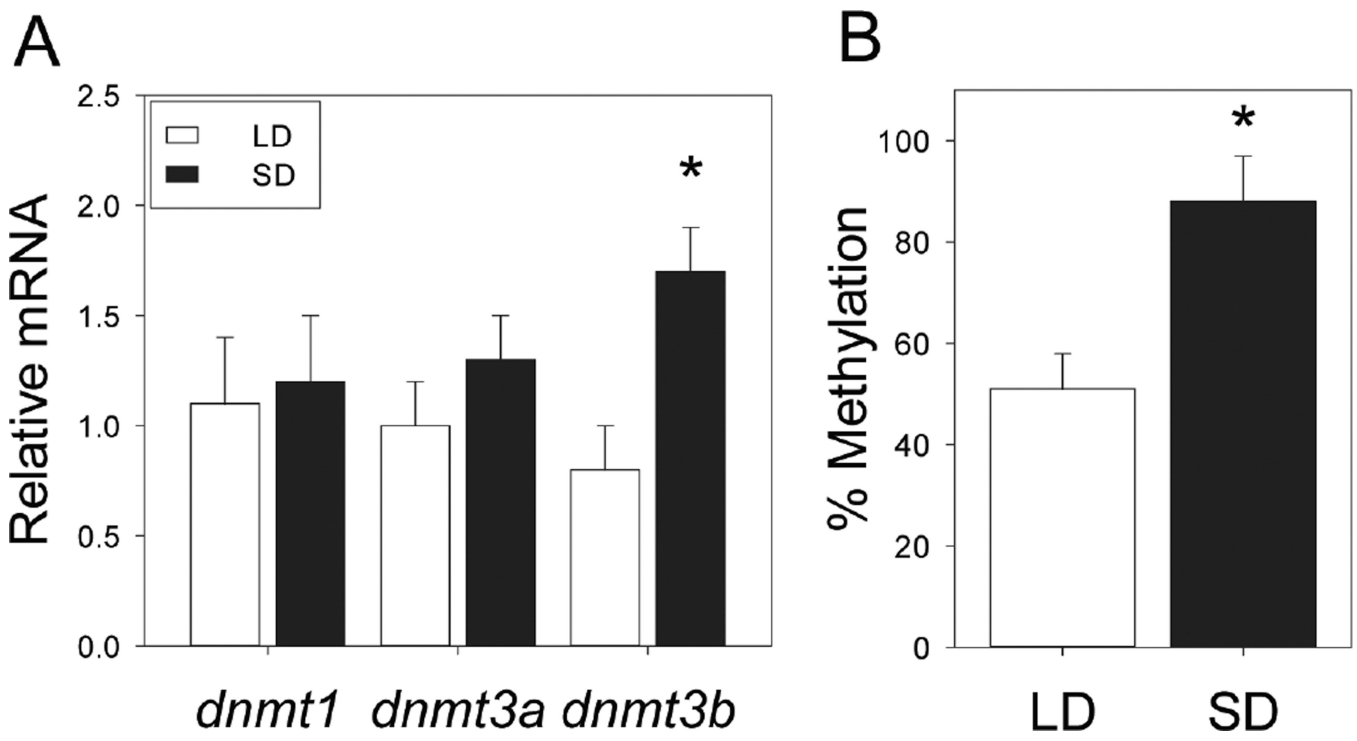

Figure 5. Short days upregulate lymphocyte DNA methyltransferase expression and increase methylation status of the *dio3* proximal promoter

(A) Mean + SEM relative levels of *dnmt1*, *dnmt3a*, and *dnm3b* mRNA expression in blood leukocytes obtained from Siberian hamsters after 10 weeks of exposure to LD and SD photoperiods. (B) Mean +SEM percentage of methylated DNA in the *dio3* proximal promoter of leukocytes obtained from LD and SD hamsters. *P<0.05 vs. LD value.

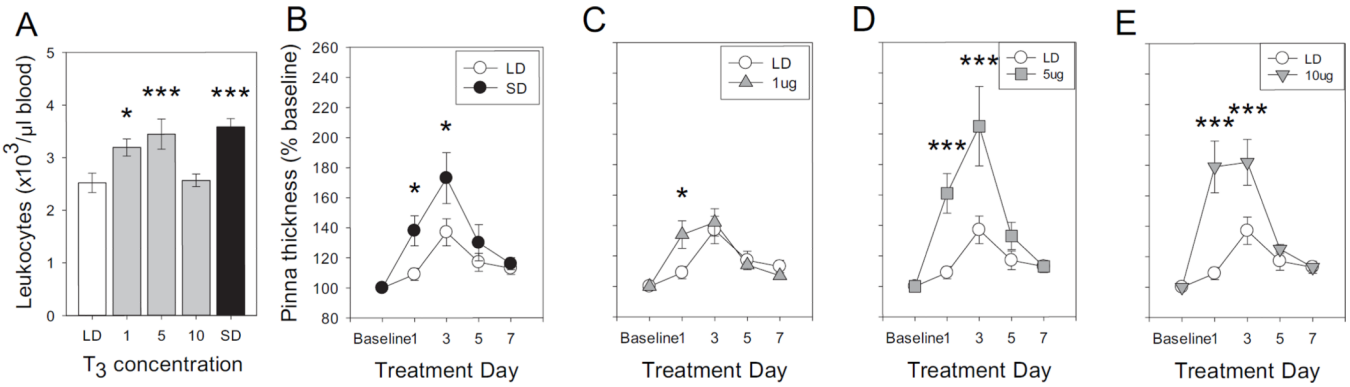

Figure 6. Exogenous T_3 mimics effects of SD on blood leukocyte concentrations and DTH inflammatory reactions

(A) Mean ±SEM blood leukocyte concentrations of Siberian hamsters housed in LD and injected daily with 1, 5, or 10 µg T_3 or saline after 3 weeks; additional controls received daily saline injections in SD. (B) Mean ±SEM DTH skin inflammatory responses in hamsters treated with T_3 or saline and LD or SD as described in Panel A. DTH was measured by ear swelling in response to antigen (DNFB) challenge delivered 1 week after antigen sensitization. *P<0.05, ***P<0.005 vs. LD value.